Institute of Experimental Morphology, Pathology and Anthropology with Museum
Bulgarian Anatomical Society

Acta Morphologica et Anthropologica, 32 (1-2)
Sofia ● 2025

Histomorphological Evaluation of Medio-Lateral Asymmetry in the Adult Murine Cerebellar Cortex

Radoslav Spasov[1], Dimo Stoyanov[1], Ivan Ivanov[2], Anton Tonchev[1]*

[1] Department of Anatomy and Cell Biology, Medical University – Varna, Varna, Bulgaria
[2] Student in Medical University – Varna, Varna, Bulgaria

***** Corresponding author e-mail: radoslav.spasov@mu-varna.bg

The cells comprising the mammalian cerebellar cortex exhibit significant variability. Individual neurons demonstrate differences regarding key parameters depending on their location within the Cerebellum`s cortical layer. We present evidence of histomorphological heterogeneity between the medial and lateral domains of the murine cerebellar cortex. Our findings show that the cerebellar cortex of normal adult mice has a surface area 42% smaller in the hemispheres compared to the Vermis and is unevenly distributed across the folia. In the Vermis, 4/10 folia constitute 55% of the total cortical surface, while in the hemispheres, 3/6 folia account for about 62%. The granule and molecular layers had lower surface area but increased thickness in the hemispheres, while the Purkinje cell layer was 46% shorter in the hemispheres compared to the Vermis. These findings advocate for caution when interpreting histomorphological changes in disease models based on the mouse cerebellum.

Key words: cerebellar cortex, molecular layer, thickness, granule layer, Purkinje cell layer

Introduction

The cerebellum is morphologically a highly complex brain region. The external morphology of the cerebellum is characterized by a plethora of sulci that mark highly branching foliations. The cerebellum is divided into one central part - vermis and two lateral parts on each side of the vermis - hemispheres. Larger fissures divide it into 3 lobes and smaller into 10 lobules, each of which contains gray and white matter [16, 18, 13]. Similar to the telencephalon, the cerebellar gray matter forms the outer aspect of the cortex, while the white matter is located deeper to the gray matter [1, 3, 5, 11, 19, 21, 22, 25]. In normal mice the Vermis contains ten folia usually denoted by numbers one to ten, while the hemispheres have six folia usually denoted by their names: Simple lobule (**LS**), crus 1 of ansiform lobule **(crus1**), crus 2 of ansiform lobule

(**crus2**), paramedian lobe (**PML**) and cupola of pyramis (**COP**), flocculonodular lobe (**FL**) [12, 15, 24]. The cortex gray matter is built by cells arranged in 3 layers: the molecular (ML), purkinje cell (PCL) and granular cell layer (GL). The classical view of the adult cerebellum states that it has a rather monotonously repetitive histological structure, but several pieces of evidence suggest that there are regional morphological differences at cellular level [7]. For example, PCs in the hemispheres have larger bodies than PCs in the Vermis [7, 17]. Granule and Golgi cells also show differences in size and packing densities between Vermis and lateral hemispheres[7, 10]. The packing density of granule cells and Purkinje cells is usually higher in the folial crowns as compared to fissures [7, 20]. Similar differences between vermis and hemispheres for the granule cells are reported across species. In this study we aim to explore if the histomorphological properties of the cerebellar cortex are constant throughout the cerebellum or there are some regional differences (between the vermis and the hemispheres). Here we show in the normal adult mouse cerebellum that not only the cell-to-cell morphological parameters exhibit regional heterogeneity but even the basic histomorphological features, such as layer thickness and surface area, are variable. These data stress that care should be taken when applying morphometric criteria to characterize cerebellar defects in mutant mouse models.

Material and Methods

Animals and tissue handling

Cerebellar tissues from normal adult mice were used from experiments following approval of the ethics committee of the state of Lower Saxony, Germany – Niedersächsische Landesamt für Verbraucherschutz und Lebensmittelsicherheit LAVES)/Oldenburg, resolution № 33.9-42502-04-11/0622 of 07.12.2011. Animals were sacrificed at P21, perfused with ice-cold 4% paraformaldehyde; the cerebellum was dissected and immersed in paraformaldehyde at 4°C. Prior to sectioning tissues were cryoprotected with PBS/Sucrose (15% and 30%), and embedded in OCT. The sections were cut at 16 μm.

Immunofluorescence

Sections were washed from the OCT in PBS, followed by antigen retrieval for 5 min at 95°C in citrate buffer. Blocking was performed with PBS/BSA/Triton for 1 hour at room temperature, primary antibodies were diluted in PBS/BSA/Triton and incubated overnight at 4°C. Secondary antibodies were incubated for 2 hours at room temperature, and DAPI was added last. Washing steps were done as needed. The following antibodies were used: to label PC, we used Calbindin manufactured by Santa Cruz with catalog number sc365360, used concentration 1:100 and Parvalbumun manufactured by Sigma Aldrich with catalog number p3088, used concentration 1:300. For secondary body we used Rabbit Thermo Fisher Scientific with catalog number A-11008, used concentration 1:300

Image acquisition

Images were acquired on a standard Leica confocal microscope with DFC 350 FX R2 camera and N PLAN 2.5x0.07 DRY objective.

Image analysis

We've done the surface measurement in Fiji (ImageJ) software using tiff files of micrographs stained with DAPI. We took the section levels for the medial micrographs at the level of the vermis, while the ones for the hemispheres were taken at the level of nucleus dentatus. We used the brush tool of Fiji for selection of the cortex/ML/GL, and subsequent creation of ROIs (regions of interest). The data was saved in the program's ROI manager as zip files. The tiff files which were calibrated (μm per pixel in accordance with the metadata of the original file). Results are presented as mm^2. To measure the thickness of ML and GL we used ROIs and generated masks from these 2 layers. Then we used the function in Fiji - Analyze -> Local Thickness -> Local Thickness "(Masked, calibrated, silent)" option. The program provided heat maps of the thickness. We further added to them calibration and scale bars. For the length of the PCL we used micrographs from staining using anti-Calbindin and anti-Parvalbumin antibodies. We used the "segmented line" of Fiji to generate the ROIs. Then we connected each of the Purkinje cells with a line which passes through the middle of each Purkinje cell and on top of the tightly packed granular cell layer without crossing the border between the layers. This is how we formed a line which we called the "Purkinje cell layer length", and measured its length.

Results

Variability of the surface area of different folia in the cerebellar Vermis and hemispheres

We started our analysis by manually segmenting the cerebellar cortex and measuring its total surface cross-sectional area (saggital levels). As expected, we found that the total area of saggital sections was significantly smaller at lateral (hemispheral) levels as compared to medial (vermal) levels: 4.414 mm^2 +/- 0.252 (lateral), 7.568 mm^2 +/- 0.342 (medial) **(Fig.1 E,** $p<0.001$**)**. This was a decrease in the surface by approx 42%. The cortical surface area showed unequal distribution across the different folia. In the Vermis, different folia surfaces ranged from 6.6% to 19.5% of the total surface area. In the hemispheres, the range was greater: from 7.3% to 28% of the total surface area **(Fig.1 C, D)**. The largest folia (IV, V, VI, IX) (4 out of 10) in the Vermis comprised 55% +/- 0.16% of the total cortical surface, while the largest folia (lobus simplex, Crus 1 of ansiform lobule and cupula of pyramid lobule) (3 out of 6) in the hemispheres composed (62% +/- 0.15%) of the total surface. The data of folia measurements are reported in **Table 1, 2 (**$p<0.001$).

Table 1. Distribution of folial surface across the cerebellum (vermis)

Folio #	**I-II**	**III**	**IV-V**	**VI**	**VII**	**VIII**	**IX**	**X**
Proportion of total Surface at this level	10.34% +/- 0.33%	10.09% +/- 0.23%	19.48% +/- 1.63%	16.78% +/- 1.15%	7.59% +/- 0.66%	10.13% +/- 0.50%	19.15% +/- 0.18%	6.43% +/- 0.27%

Table 2. Distribution of folial surface across the cerebellum (hemispheres)

Folial name	LS	Crus1	Crus 2	PML	COP	FLN
Proportion of total Surface at this level	19.29% +/- 0.39%	27.69% +/- 2.23%	09.25% +/- 0.49%	11.91% +/- 1.45%	24.27% +/- 0.66%	07.39% +/- 0.19%

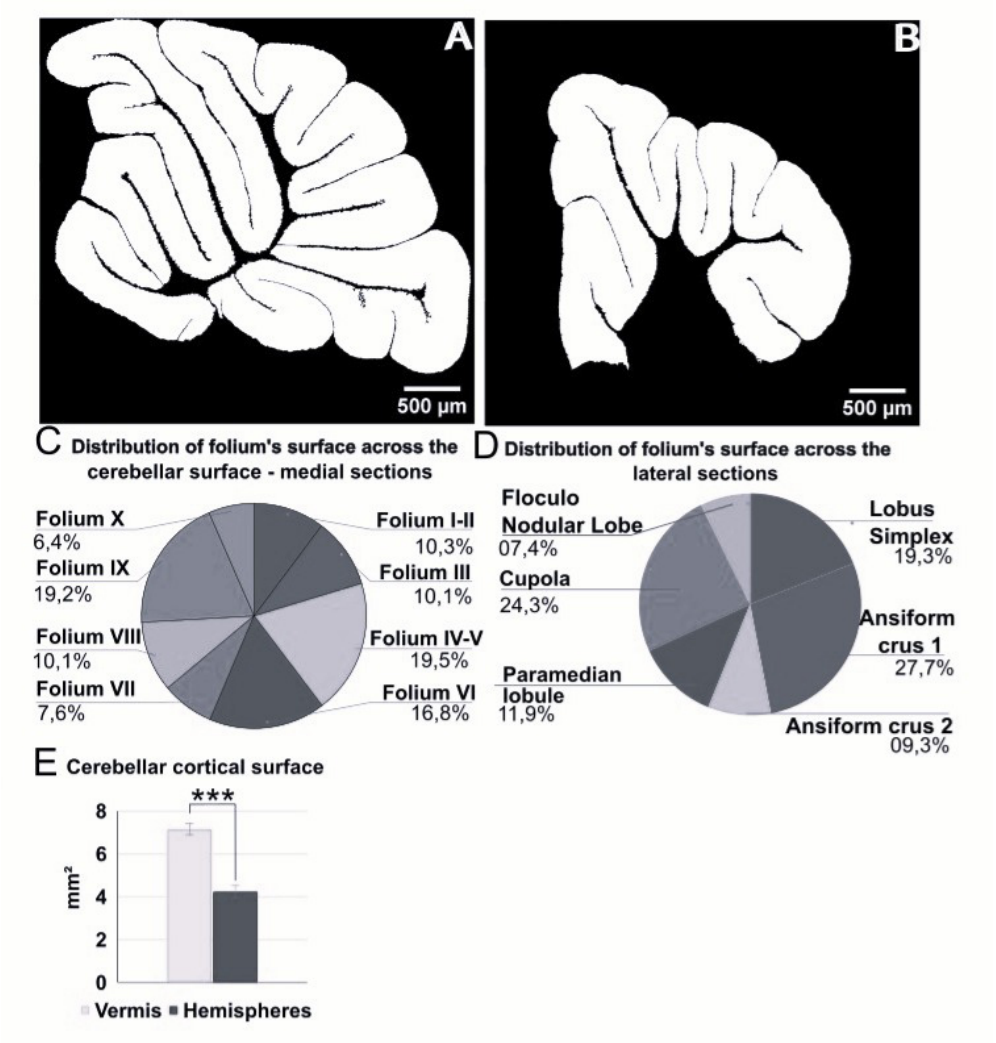

Fig. 1. Surface area of the cerebellar cortex and proportions of the area of individual folia out of the total surface. **(A)** and **(B)**: digital masks; **(E)**: diagram that represents the cerebellar cortical surface, ***p<0.001; **(C)** and **(D)**: pie charts showing the representation of the surface of individual cerebellar folium from the total surface area in vermis and hemispheres, ***p<0.001.

Variability of surface area of ML and GL in the Vermis and hemispheres

We investigated the surface area of individual layers in medial and lateral anatomical levels of the adult cerebellum. To this aim, we studied the areas of ML and GL across the entire section of the cerebellar foliation. We performed the measurements following a manual segmentation of the ML and GL (**Fig. 2, 3**). We estimated the total surface of the ML at 3.791 mm^2 +/- 0.139 in the vermis and 2.274 mm^2 +/- 0.107 in the hemispheres (**Fig. 2C**, $p<0.001$). We estimated the total surface of the GL at 3.374 mm^2 +/- 0.132 in the vermis vs 1.968 mm^2 +/- 0.183 in the hemispheres (**Fig. 3C**, $p<0.001$). The proportion of the reduction of the total surface of ML and GL in the hemispheres as compared to the Vermis was similar, approx. 40%.

We next measured the thickness of the ML and GL. Unlike the areal measurements, the estimations of the thickness demonstrated that both layers were thicker in the hemispheres as compared to the Vermis. The average ML thickness in the Vermis was 125.555 µm +/- 3.289, while in the hemispheres it was 149.629 µm +/- 3.412 (**Fig. 2D**, $p<0.001$). The average GL thickness in the Vermis was 121.863 µm +/- 4.102, while in the hemispheres it was 140.606 µm +/- 7.782 (**Fig. 3D**, $p<0.01$). Thus, the ML was thicker by approx 20% in the hemispheres while the GL thickness increased by approx. 15%.

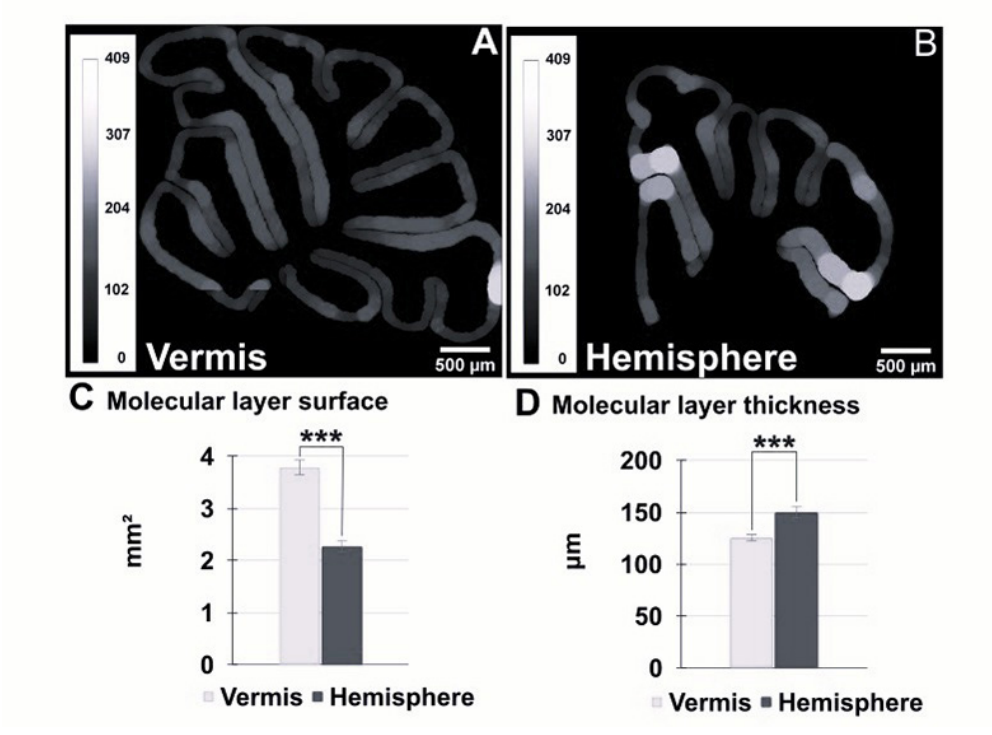

Fig. 2. Surface area and local thickness of the cerebellar molecular layer. **(A)** and **(B)**: heat maps that represent the surface area and the local thickness of the molecular layer; **(C)** and **(D)**: diagrams of surface and local thickness of the cerebellar molecular layer in the vermis and hemispheres, *** $p<0.001$.

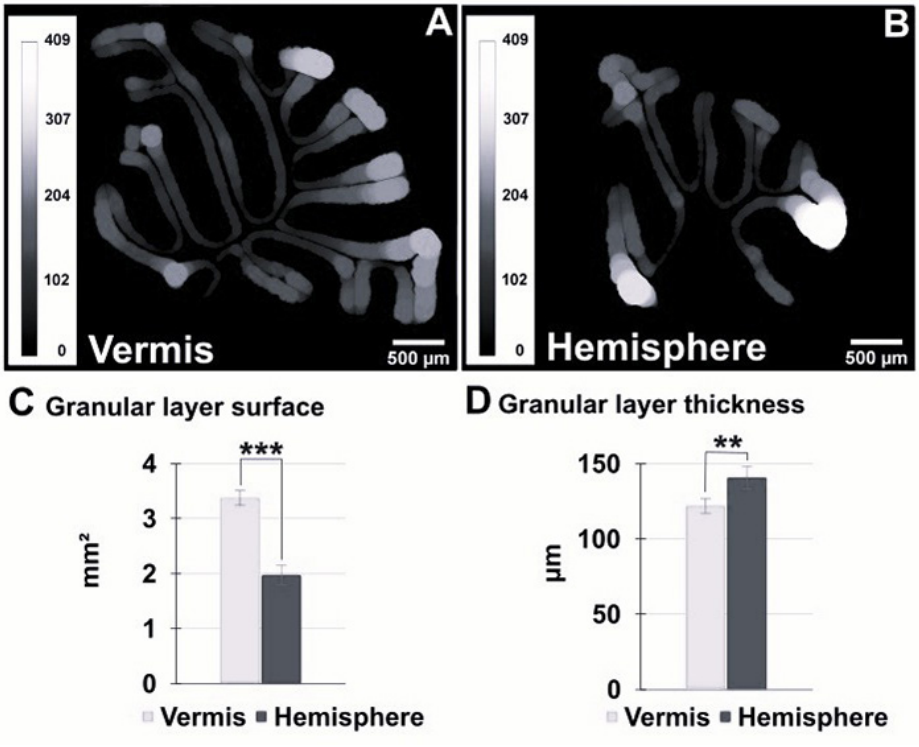

Fig. 3. Surface area and local thickness of the cerebellar granular layer. **(A)** and **(B)**: heat maps that represent the surface area and the local thickness of the granular layer; **(C)** and **(D)**: diagrams of the surface and local thickness of the cerebellar granular layer in vermis and hemispheres, *** $p<0.001$, ** $p<0.01$.

We also measured the length of the PCL (**Fig. 4**). In the vermis was 30.399 mm +/- 4.102 vs 16.048 μm^2 +/- 0.939 in the hemispheres (**Fig. 4C**, $p<0.001$). Again, here we observed a decrease in the total length by nearly half – 46% in the hemispheres compared to the vermis.

Discussion

This is the first study showing the regional differences (between Vermis and hemispheres) in the surface area and the thickness of the cortex and its components, as well as the length of the Purkinje cell layer. The first main goal of our study was to compare the cerebellar cortical surface in the Vermis and hemispheres. Recent data show differences in the packing densities and cell size for different cell subpopulations (PC, Golgi neurons, granule cells) in the Vermis versus hemispheres**.** Here we aimed to explore whether this applies to its general morphometric description. First, we found that the total area of the cortex is more evenly spread in between the folia of the vermis compared to the hemispheres. More precisely the range between the smallest

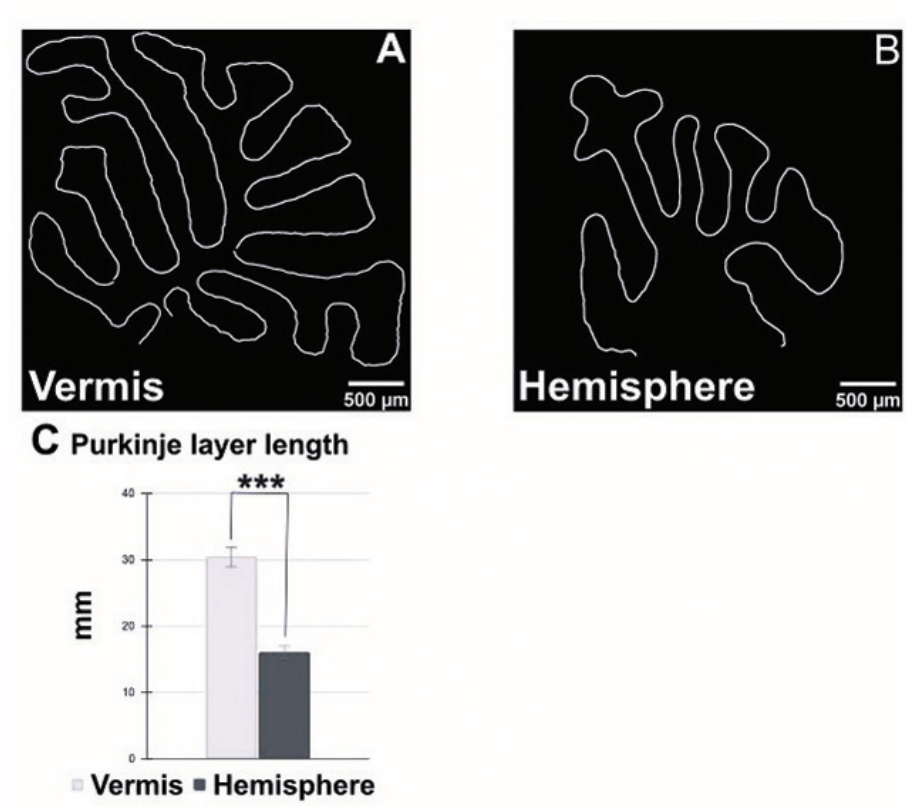

Fig. 4. Length of Purkinje cell layer. **(A)** and **(B)**: lines that represent the Purkinje cell layer length; **(C)**: diagram of the length in the Purkinje cell layer in Vermis and hemispheres, ***p<0.001.

and biggest folium, as a percent of the total area, was 12.8% for the vermis versus 20.3% for the hemispheres. Our measurements in the Purkinje cell layer length show a severe decrease. That is indicative of the total cortical length and foliation complexity. Interestingly the cerebellar cortex is thicker overall in the hemispheres. This increase in thickness is due to thickening of both the ML and GL, thus the ML/GL thickness ratio is preserved. Our observations confirm previous studies [4, 7] describing that folium crowns have thinner cortices compared to the grooves. This is accompanied by a more densely packed PC and granule cells in the crown regions [2,4 , 7]. The general thickening of the cortex in the hemispheres as compared to the Vermis might indicate of the existence of regional differences in cell density and ultrastructural morphology.

Conclusions

Changes in the cerebellar cytoarchitecture occur in various conditions [6, 8, 9, 14, 23]. In one of them – the autistic spectrum disorder (ASD) may reflect a disruption in neuronal networks during development [26, 27]. Our results suggest that the following

morphometric criteria might be used when evaluating morphological changes in different models: (i) the PCL length and cortical surface; (ii) the precise anatomical level (i.e. measurements should be performed at both medial and lateral levels); (iii) quantification of individual layers (i.e. measuring surface and thickness of the GL and ML); (iv) the proportion of each folium out of the total area at any given anatomical level. We hope our results might be helpful in providing a more comprehensive and structured workflow for morphological assessment of the adult cerebellum.

Acknowledgement: This work was funded by the "Science" Fund of the Medical University – Varna, project #20029.

References

1. **Amaral, D. G., M. P. Witter.** The three-dimensional organization of the hippocampal formation: A review of anatomical data. – *Neuroscience,* **31**, 1989, 571–591.
2. **Armstrong, D. M., R. F. Schild**. A quantitative study of the purkinje cells in the cerebellum of the albino rat. – *J. Comparative Neurology,* **139**, 1970, 449-456.
3. **Au, W. W., H. B. Treloar, C. A. Greer**. Sublaminar organization of the mouse olfactory bulb nerve layer. – *J. Comparative Neurology,* **446**, 2002, 68-80.
4. **Braitenberg, V., R. P. Atwood**. Morphological observations on the cerebellar cortex. – *J. Comparative Neurology,* **109**, 1958, 1-33.
5. **Briscoe, S. D., C. W. Ragsdale**. Evolution of the chordate telencephalon. – *Current Biology,* **29**, 2019, R647–R662.
6. **Campbell, D. B., J. B. North, E.J. Hess**. Tottering mouse motor dysfunction is abolished on the Purkinje cell degeneration (pcd) mutant background. – *Experimental Neurology*, **160**, 1999, 268-278.
7. **Cerminara, N. L., E. J. Lang, R. V. Sillitoe, R. Apps.** Redefining the cerebellar cortex as an assembly of non-uniform Purkinje cell microcircuits. – *Nat. Rev. Neurosci.*, **16**, 2015, 79-93.
8. **Danielian, P. S., A. P. McMahon**. Engrailed-1 as a target of the Wnt-1 signalling pathway in vertebrate midbrain development. – *Nature*, **383**, 1996, 332-334.
9. **Engelkamp, D., P. Rashbass, A. Seawright, V. V. Heyningen.** Role of Pax6 in development of the cerebellar system. – *Development*, **126**, 1999, 3585-3596.
10. **Geurts, F. J., J.-P. Timmermans, R. Shigemoto, E. De Schutter.** Morphological and neurochemical differentiation of large granular layer interneurons in the adult rat cerebellum. – *Neuroscience,* **104**, 2001, 499-512.
11. **Guillemot, F**. Cellular and molecular control of neurogenesis in the mammalian telencephalon. - *Current Opinion in Cell Biology*, **17**, 2005, 639-647.
12. **Heuer, K., N. Traut, A. A. De Sousa, S. L. Valk, J. Clavel, R. Toro**. Diversity and evolution of cerebellar folding in mammals. – *eLife,* **12**, 2023, e85907.
13. **Hull, C., W. G. Regehr**. The Cerebellar cortex. – *Annu. Rev. Neurosci,* **45**, 2022, 151-175.
14. **Isaacs, K. R., L. C .Abbott**. Cerebellar volume decreases in the tottering mouse are specific to the molecular layer. - *Brain Research Bulletin*, **36**, 1995, 309-314.
15. **Kozareva, V., C. Martin, T. Osorno, S. Rudolph, C. Guo et al**. A transcriptomic atlas of mouse cerebellar cortex comprehensively defines cell types. – *Nature*, **598**, 2021, 214-219.

16. **Lara-Aparicio, S. Y., A. J. Laureani-Fierro, C. Morgado-Valle, L. Beltran-Parrazal, F. Rojas-Duran et al**. Latest research on the anatomy and physiology of the cerebellum. – *Neurology Perspectives,* **2**, 2022, 34-46.
17. **Lange, W.** Regional differences in the distribution of golgi cells in the cerebellar cortex of man and some other mammals. – *Cell Tissue Res*, **153**, 1974.
18. **Marzban, H., M. R. Del Bigio, J. Alizadeh, S. Ghavami, R. M. Zachariah, M. Rastegar.** Cellular commitment in the developing cerebellum. – *Front. Cell Neurosci*., **8**, 2015.
19. **Meek, J.** Functional anatomy of the tectum mesencephali of the goldfish. An explorative analysis of the functional implications of the laminar structural organization of the tectum. – *Brain Research Reviews*, **6**, 1983, 247-297.
20. **Muller, U., H. Heinsen**. Regional differences in the ultrastructure of Purkinje cells of the rat. – *Cell Tissue Res,* **235**, 1984.
21. **Nagayama, S., R. Homma, F. Imamura**. Neuronal organization of olfactory bulb circuits. – *Front. Neural Circuits,* **8**, 2014.
22. **Nevin, L. M., E. Robles, H. Baier, E. K. Scott**. Focusing on optic tectum circuitry through the lens of genetics. – *BMC Biol.,* **8**, 2010, 126.
23. **Rossman, I. T., E. DiCicco-Bloom**. Engrailed2 and cerebellar development in the pathogenesis of autism spectrum disorders. In: *Autism. Current theories and evidence*. (Ed. A. W. Zimmerman), Humana Press/Springer Nature, 2008, 3-40.
24. **Ullmann, J. F. P., M. D. Keller, C. Watson, A. L. Janke, N. D. Kurniawan et al**. Segmentation of the C57BL/6J mouse cerebellum in magnetic resonance images. – *NeuroImage* **62**, 2012, 1408-1414.
25. **Witter, M. P., F. G. Wouterlood, P. A. Naber, T. Van Haeften**. Anatomical organization of the parahippocampal-hippocampal network. – *Annals of the New York Academy of Sciences*, **911**, 2000, 1–24.
26. **Zhelezov, M.** Microglia as potential regulators of empathy and prosocial behavior – A hypothesis. – *Biomedical Reviews*, **27**, 2017, 69.
27. **Zhelezov, M.** Microglial adipobiology: a new concept for understanding the adipose tissue-brain crosstalk in health and disease. – *Adipobiology*, **10**, 2019, 25.